Biogeosciences

Open Access

Biogeochemical origins of particles obtained from the inversion of the volume scattering function and spectral absorption in coastal waters

X. Zhang[1], Y. Huot[2], D. J. Gray[3], A. Weidemann[4], and W. J. Rhea[3]

[1]Earth System Science and Policy, University of North Dakota, Grand Forks, North Dakota 58202, USA
[2]Centre d'applications et de recherches en télédétection, Université de Sherbrooke, Sherbrooke, QC J1K 2R1, Canada
[3]US Naval Research Laboratory Code 7231, Washington, DC 20375, USA
[4]US Naval Research Laboratory Code 7330, Stennis Space Center, MS 39529, USA

Correspondence to: X. Zhang (zhang@aero.und.edu)

Abstract. In the aquatic environment, particles can be broadly separated into phytoplankton (PHY), non-algal particle (NAP) and dissolved (or very small particle, VSP) fractions. Typically, absorption spectra are inverted to quantify these fractions, but volume scattering functions (VSFs) can also be used. Both absorption spectra and VSFs were used to estimate particle fractions for an experiment in the Chesapeake Bay. A complete set of water inherent optical properties was measured using a suite of commercial instruments and a prototype Multispectral Volume Scattering Meter (MVSM); the chlorophyll concentration, [Chl] was determined using the HPLC method. The total scattering coefficient measured by an ac-s and the VSF at a few backward angles measured by a HydroScat-6 and an ECO-VSF agreed with the LISST and MVSM data within 5 %, thus indicating inter-instrument consistency. The size distribution and scattering parameters for PHY, NAP and VSP were inverted from measured VSFs. For the absorption inversion, the "dissolved" absorption spectra were measured for filtrate passing through a 0.2 μm filter, whereas [Chl] and NAP absorption spectra were inverted from the particulate fraction. Even though the total scattering coefficient showed no correlation with [Chl], estimates of [Chl] from the VSF-inversion agreed well with the HPLC measurements ($r = 0.68$, mean relative errors $= -20$ %). The scattering associated with NAP and VSP both correlated well with the NAP and "dissolved" absorption coefficients, respectively. While NAP dominated forward, and hence total, scattering, our results also suggest

that the scattering by VSP was far from negligible and dominated backscattering. Since the sizes of VSP range from 0.02 to 0.2 μm, covering (a portion of) the operationally defined "dissolved" matter, the typical assumption that colored dissolved organic matter (i.e., CDOM) does not scatter may not hold, particularly in a coastal or estuarine environment.

1 Introduction

The interaction of light with aquatic particles alters the spectral and angular characteristics of the incident light field. Inversion approaches in ocean optics are based on our understanding of these interactions, which allow water constituent properties to be inferred from measurements of the light field. Solutions to inverse problems include single particle (e.g., Green et al., 2003) as well as globe scale (e.g., Siegel et al., 2005) applications. In clear oceanic waters, phytoplankton and their decay byproducts are the predominant sources of optical variability (Morel, 1988; Morel and Maritorena, 2001; Gordon et al., 1988). In coastal waters with the presence of particles of various types and origins, each playing a potentially significant optical role (Babin et al., 2003; Morel and Prieur, 1977), it is particularly challenging to link the measured light field to optically active water constituents and their biogeochemical origins.

The inherent optical properties (IOPs; Preisendorfer, 1976) of particulate matter provide the fundamental link be-

tween the biogeochemical and optical properties of particle populations. In contrast to apparent optical properties, which also depend on the angular distribution of the incident light field, the IOPs depend only on the nature and concentration of the particles, and thus require fewer assumptions or ancillary measurements to solve the inverse problems. Ignoring inelastic scattering, there are two fundamental inherent optical properties: the absorption coefficient (a, m^{-1}) and the volume scattering function (VSF, m^{-1} sr^{-1}). The total scattering coefficient (b, m^{-1}) and the backscattering coefficient (b_{b}, m^{-1}) can be derived from the VSF by integration over the appropriate angles. The sum of the absorption and scattering coefficients is the attenuation coefficient (c, m^{-1}).

Absorption by particles in the ocean is largely isotropic (i.e., no directional preference); it is the spectral variations of absorption that are generally used for inferring information about water constituents. Two main classes of particles are generally distinguished when interpreting the bulk absorption characteristics of substances present in the water: non-algal matter (NAM), sometimes also referred to as detrital matter, and phytoplankton cells (Sathyendranath et al., 1989; Babin et al., 2003; Magnuson et al., 2004). Putting aside microbes using bacteriochlorophylls and rhodopsin-based photosynthesis, all photosynthesizing microbes contain chlorophyll a (including divinyl chlorophyll a) and show a characteristic absorption peak near 676 nm and a broader peak centered near 440 to 445 nm. Note, however, that individual spectra can exhibit considerable variability (Bricaud et al., 1998; Ciotti et al., 2002). Spectral absorption by NAM, organic or inorganic, generally has a decreasing exponential shape with respect to wavelength in the visible range (Wozniak and Dera, 2007). Spectra for mineral particles often have absorption shoulders caused by certain elements (Babin and Stramski, 2004); in small amounts, however, they are generally difficult to distinguish, based only on their absorption characteristics, from the organic portion of NAM (also see Estapa et al., 2012). Analytically, NAM is often separated by filtration through a 0.2 µm filter into two fractions: the dissolved fraction referred to as colored dissolved organic matter (CDOM) and the particulate fraction referred to as the non-algal particulates (NAP). This division, indeed, is a matter of convention and the "dissolved" fraction also contains "undissolved" particles, which we refer to as very small particles (VSP) (Stramski et al., 2001).

Like absorption, there are variations in the spectral shape of scattering (e.g., Doxaran et al., 2009; Gould et al., 1999), which have been used to infer the slope of the bulk particle size distribution in the ocean (Boss et al., 2001; Morel, 1973). However, a significant amount of information about particles can be derived from its angular distribution, often called the volume scattering function (VSF). For example, the backscattering ratio (fraction of scattered light into the backward directions) has been used to infer the bulk refractive index of particles (Twardowski et al., 2001; Boss et al., 2004). Measurements of VSFs at near forward angles, from

commercial instruments, have been used to derive the size distribution of larger particles ($\sim$ 2 to 200 µm) (Chin et al., 1955; Coston and George, 1991; Knight et al., 1991; Riley and Agrawal, 1991). Building on earlier studies (Gordon and Brown, 1972; Zaneveld et al., 1974), Zhang et al. (2011) developed an inversion method that uses the full angular range of VSFs to retrieve the size and composition of particles. In the inversion, the measured particle VSFs are disaggregated into fractional contributions by particle subpopulations. The VSF-inversion method has been evaluated in several studies with promising results. For waters south of Hawaii, the size distribution of microbubbles inverted from the measured VSFs agreed well with concurrent acoustical results (Czerski et al., 2011). In the surf zone off of Scripps Pier, the wave-injected bubble and suspended sediment populations derived from the VSF-inversion were found to be consistent with acoustical measurements of bubbles and video observations of mineral particles, respectively (Twardowski et al., 2012). In three coastal water locations in the United States with complex particle populations, Zhang et al. (2012) compared the bulk particle size distributions derived from the VSFs and the commercial LISST instrument; they found differences of less than 10 % for radiuses from 1 to 100 µm. They also showed that chlorophyll concentrations estimated from inverted particle sub-populations (with refractive indices of 1.04–1.06 and radiuses of 0.2–100 µm) covaried with in situ measured chlorophyll concentrations during an observed phytoplankton bloom event in the Chesapeake Bay.

Spectral absorption has been routinely measured in the field (Yentsch, 1962), whereas only a few datasets of VSFs have been published in the past (Petzold, 1972; Kullenberg, 1968). It is only recently that more datasets have been measured (Chami et al., 2005; Berthon et al., 2007; Sullivan and Twardowski, 2009) due to the development of two new prototype angular scattering sensors, the Multispectral Volume Scattering Meter (MVSM or VSM) (Lee and Lewis, 2003) and the Multi-Angle Scattering Optical Tool (MASCOT) (Twardowski et al., 2012). In the present study, a field experiment in Chesapeake Bay with concurrent measurements of spectral absorption and angular scattering provided an opportunity to examine the biogeochemical sources of both absorption and scattering.

2   Data and methodology

In this study, the pure water or seawater contribution has been removed from all of the IOP measurements; the subscript "nw" indicates the non-water portion of IOPs. To be consistent with our previous work, we used the (equivalent) radius to describe the size of particles inferred from the inversion. A filter with a 0.2 µm pore size would allow particles with a radius of approximately 0.1 µm or less to pass through. Except for the volume scattering function with units of m^{-1} sr^{-1}, all other IOPs describes herein have units of m^{-1}.
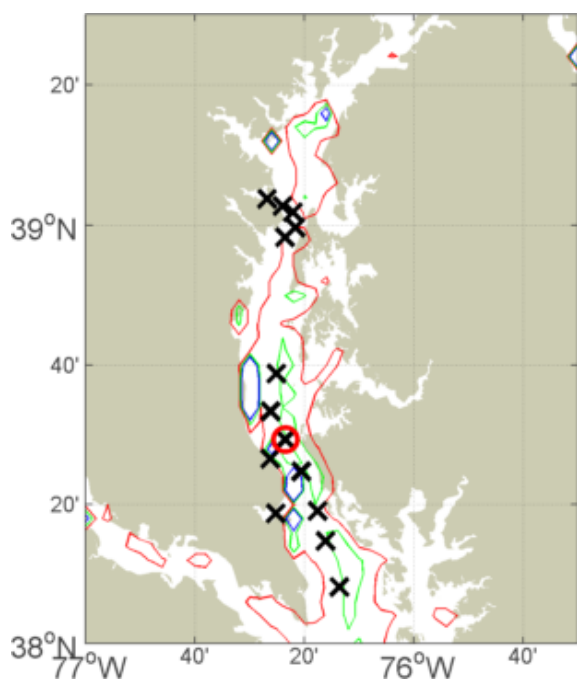
Fig. 1. The sampling locations and bathymetry (red, green and blue contours: 5, 15 and 25 m water depths) in the Chesapeake Bay. The circle highlights station CB3, for which inversion results are shown in Fig. 4.

2.1 Field experiment

The experiment took place in Chesapeake Bay between the 12 and 22 October 2009 (Fig. 1). Chesapeake Bay is a large estuary with considerable and varied freshwater inputs. Particles in the water cover a wide spectrum including: terrigenous, resuspended sediments, phytoplankton, and non-algal matter of organic origin. Between the 15 and 18 October 2009, radar measurements showed the Chesapeake Bay watershed received around 90 mm of rain, which interrupted the experiment. The following few days had relatively clear skies, and an algal bloom was observed at the sampling stations in the middle of the bay.

A suite of instruments was deployed, including a CTD (Sea-Bird Electronics, Inc., WA), ac-s, ac-9, ECO-VSF, WETstar (all by WETLabs, Inc., OR), HydroScat-6 (HS6, Hobi Labs, Inc., AZ), LISST-100X (Type B; Sequoia, Inc., WA) and MVSM. In addition, water samples were collected for laboratory analysis. All the instruments were deployed at the same time and location but in four different packages. The HS6, LISST and MVSM were deployed separately while the CTD, ac-s, ac-9, ECO-VSF and WETstar were in the same package. Except for the MVSM, which recorded continuously at the surface, all the other instruments took profiles of the water column. The profile data were binned; the binned data at or closest to the MVSM depth were used in this study.

2.2 Volume scattering functions

The volume scattering function was measured using three commercial instruments (the ECO-VSF, the HydroScat-6 and the LISST-100) as well as one prototype scattering meter, the Multispectral Volume Scattering Meter (MVSM).

The ECO-VSF measures the VSF at 100°, 125° and 150° at 470, 530 and 660 nm. During the deployments, the 100° and 125° channels were incorrectly calibrated, and we were not able to obtain accurate values at those angles (James Sullivan, personal communication, 2013); they are not presented here. The HydroScat-6 (HS6) measures the VSF at 140° at six wavelengths (420, 442, 470, 510, 590 and 700 nm). Both ECO-VSF and HS6 data were processed following the manufacturers' protocols, WET Labs ac Meter Protocol Document (Rev. M) and HOBILabs HydroScat-6 Spectral Backscattering Sensor User's Manual (Rev E), respectively, using the default settings.

The LISST-100X that we used operates at 532 nm, and measures VSFs at angles from 0.07 to 13.9°. To reduce the ambient light contamination, the instrument was deployed vertically with its sensor looking down rather than the normal horizontal position (Zhang et al., 2012). The data collected during a cast were averaged and binned into 0.5 m depth intervals. The VSF was calculated following Slade and Boss (2006), and the scattering angles were calculated based on the instrument and detector geometry.

The MVSM operates at eight wavelengths (443, 490, 510, 532, 555, 565, 590, and 620 nm) with a spectral band-pass of 9 nm. It measures VSFs at an angular resolution of 0.25° from 0.5 to 179°. One complete MVSM run takes approximately 10 min. In the field, the instrument was held at a constant near-surface depth of about 1.5 m with ambient water pumped at 2 to 3 L per minute through the sample chamber using a SeaBird 5T pump placed at the outlet. For each station, we collected two complete sets of VSFs, from which an average was computed. This average was then processed following Berthon et al. (2007) to obtain the VSF.

The final VSFs were determined by combining the 532 nm MVSM data at angles greater than 9.5° with the LISST data binned at the corresponding MVSM depth for angles up to 9.48°. This procedure was intended to address two issues (Zhang et al., 2012): (1) problematic measurements by the MVSM that were found at angles less than 10° during laboratory tests with polystyrene beads, and (2) the residual ambient light contamination that was still present primarily at the two largest angles of the LISST when the instrument was near the surface. Since each instrument was calibrated in terms of the absolute geophysical unit of VSF (m^{-1} sr^{-1}), no scaling was applied to the data from either instrument; the data were simply merged based on their angles. The VSF of pure seawater was estimated using the Zhang et al. (2009) model and subtracted from the final VSFs. Note that the MVSM data at other wavelengths, though not used in the inversion, were used for comparison with the HS6 data.

2.3 Absorption coefficient

The attenuation and absorption coefficients were measured using an ac-s and an ac-9. A 0.2 μm AcroPak 1000 cartridge filter (Pall Co., NY) was attached to the intake tube of the ac-9's a-meter. The corrections for temperature and salinity (Sullivan et al., 2006) were applied to both measurements. The measured absorption and attenuation spectral values for pure water were subtracted from the measurements. With these corrections, the ac-s data provided estimates of non-water attenuation, c'_{nw}, and non-water absorption, a'_{nw}, and the ac-9 data provided estimates of the absorption due to colored dissolved organic matter, a'_{CDOM}. In addition, the a'_{CDOM} data interpolated at the ac-s wavelengths were subtracted from the ac-s's c'_{nw} and a'_{nw}, providing estimates of particulate attenuation coefficient c'_p and absorption coefficient a'_p. It is well understood that the attenuation and absorption coefficients (c' and a') thus estimated are respectively lower and higher than the corresponding "true" values (c and a), because the 0.93° acceptance angle of the c-meter also measures near-forward scattering (Boss et al., 2009) while a portion of light that is scattered backward is included in absorption measurements (Zaneveld et al., 1994). The value of a'_{CDOM} at 715 nm (assumed to be due to scattering) was subtracted from a'_{CDOM} spectra to estimate a_{CDOM} (e.g., Babin et al., 2003; Magnuson et al., 2004). Zaneveld et al. (1994) method was applied to c'_p and a'_p to estimate a_p. When deriving absorption coefficients, a major uncertainty is the near infrared wavelength used as a reference in the scattering correction method. The assumption that absorption due to CDOM and particulates is negligible at 715 nm may not hold in our study area (e.g., Doxaran et al., 2007). However, despite these uncertainties, a recent study shows that the Zaneveld method using 715 nm as the reference performs reasonably well (Leymarie et al., 2010).

To obtain an estimate of non-algal particle absorption, the a_p was further partitioned into contributions by phytoplankton and by non-algal particles (NAP) using a simple spectral inversion (nonlinear least squares fit between the measurement and the model) based on the following relationship:

$$\begin{aligned} a_p(\lambda) &= a_{PHY}(\lambda) + a_{NAP}(\lambda) \\ &= [\text{Chl}]_{ac\text{-}s}(S_f a^*_{pico}(\lambda) + (1 - S_f)a^*_{micro}(\lambda)) \\ &\quad + a_{NAP}(400)e^{-S_{NAP}(\lambda - 400)} \end{aligned} \quad (1)$$

In Eq. (1), $a_{PHY}(\lambda)$ and $a_{NAP}(\lambda)$ are respectively the phytoplankton and the NAP absorption coefficients. The phytoplankton absorption coefficient is represented as the product of the chlorophyll concentration ([Chl], mg m^{-3}) and the chlorophyll specific absorption coefficient, with the latter estimated as a linear mixing of two phytoplankton species that represent end members for the specific absorption values, a^*_{pico} (m^2 mg chl^{-1}) for picoplankton and a^*_{micro} (m^2 mg chl^{-1}) for microplankton following Ciotti et al. (2002). In this parameterization, S_f (dimensionless) rep-

resents the fraction of picoplankton in the sample. The absorption by NAP is modeled as an exponentially decreasing function with a reference value of $a_{NAP}(400)$ at 400 nm and an exponential slope of S_{NAP} (nm^{-1}). We used a bounded least squares method to simultaneously estimate [Chl]$_{ac\text{-}s}$, S_f, $a_{NAP}(400)$ and S_{NAP}. Bounds were set such that the solutions had to be within the following ranges: $0 < [\text{Chl}]_{ac\text{-}s} < 60$ mg m^{-3}, $0 < S_f < 1$, $0 < a_{NAP}(400) < 5$ m^{-1}, $0.006 < S_{NAP} < 0.012$ nm^{-1}. The bounds set for S_{NAP} were based on the observations of Magnuson et al. (2004) in Chesapeake Bay whereas the bounds for [Chl]$_{ac\text{-}s}$ and $a_{NAP}(400)$ were set to be sufficiently high based on in situ data to avoid an artificial ceiling. The fit was carried out between 401 and 713 nm; we omitted the region between 525 and 602 nm because we observed a strong absorption peak likely originating from phycobilins, which is not present in our two extreme spectra. Only $a_{NAP}(400)$ and [Chl]$_{ac\text{-}s}$ are reported here, but it is worth noting that the retrieved S_f were always smaller than 0.07, which is consistent with the presence of highly packaged cells, and that $a_{PHY}(443)$ ranged from 8 to 50 % of the total non-water absorption with an average of 30 %. We also note (not shown) that the [Chl]$_{ac\text{-}s}$ retrieved with this method showed a correlation coefficient of 0.99 with the baseline method (Boss et al., 2007).

2.4 VSF inversion

The theoretical background for general inversion techniques can be found in Twomey (1977). The technical details for the VSF-inversion were reported in Zhang et al. (2011, 2012). In this study, the VSF inversion was performed following Zhang et al. (2012). Briefly, the non-water VSF, $\beta_{nw}(\theta)$ (m^{-1} sr^{-1}), where θ is the scattering angle, is decomposed into the contributions ($\beta_i(\theta)$) by M particle subpopulations; this is accomplished through inversion based on a prescribed kernel function $\bar{\beta} = [\bar{\beta}_1, \bar{\beta}_2, \ldots, \bar{\beta}_M]$, where $\bar{\beta}_i$ ($i = 1$ to M) (sr^{-1}) is the scattering phase function for the particle subpopulation i. Each particle subpopulation is uniquely represented by three parameters: the refractive index (n_i), the mode size (r_{mode_i}, μm) and the standard deviation (σ_i, unitless). The refractive index is closely related to the composition or the type of particles (Aas, 1996; Carder et al., 1974). The mode size and the standard deviation describe a log-normal distribution, which has been found to represent natural particle species in the aquatic environment very well (Lambert et al., 1981; Campbell, 1995; Vaillancourt and Balch, 2000; Peng and Effler, 2010). In computing the kernel function, the particles (except for bubbles, which are assumed spherical) were assumed to have an asymmetric hexahedral shape. Real oceanic particles are in general nonspherical and cannot be represented simply by a single shape. The reason we chose asymmetric hexahedral shape is because it has been shown to simulate well the optical properties and polarization states of mineral aerosol particles, which do not possess a particular

shape either (Bi et al., 2010). Altogether, one set of the VSFs measured at 709 angles is inverted for particle subpopulations from approximately 90 ($M = 92$) optically distinctive candidates, with r_{mode} varying from $0.01 \sim 10\,\mu\text{m}$, σ from $0.1 \sim 1.1$, and n from 0.75 (for bubbles) to 1.2. The final output of the VSF inversion includes the scattering coefficient, b_i (m^{-1}), and the number concentration, N_i (m^{-3}), for each subpopulation, i.e., $\beta_i(\theta) = b_i \bar{\beta}_i(\theta)$ and $b_i = N_i C_{sca,i}$, where $C_{sca,i}$ (m^2) is its average scattering cross-sectional area.

The inverted subpopulations were then grouped into three categories. Very small particles (VSP) represent those subpopulations with r_{mode_i} less than $0.1\,\mu\text{m}$. Since the smallest mode size assumed in the inversion is $0.01\,\mu\text{m}$, the VSP thus corresponds roughly to the dissolved particles of sizes from 0.02 to $0.2\,\mu\text{m}$ based on filtration with a pore size of $0.2\,\mu\text{m}$ or to small colloidal particles (Stramski and Wozniak, 2005). The non-VSP subpopulations were divided into two groups: phytoplankton (PHY) including particles whose refractive index is between 1.03 and 1.08 (Aas, 1996, see also Fig. 3), and non-algal particles (NAP) representing everything else. Therefore, $b_{nw} = b_{VSP} + b_{PHY} + b_{NAP}$ and $b_{bnw} = b_{bVSP} + b_{bPHY} + b_{bNAP}$, where the subscripts refer to the particle types mentioned above. In reality, these fractions may not always partition constituents according to their biogeochemical properties. For example, some NAP could have a refractive index of 1.05. But, from a modeling point of view, a phytoplankton-type particle and a NAP with a similar refractive index and size would behave similarly in terms of their angular scattering. This is a limitation of the VSF inversion. Heterotrophic bacteria are another example of a limitation of the approach. With radii near $0.2\,\mu\text{m}$ and refractive indices around 1.05 (Stramski et al., 2001), such particles, which are part of the NAP, would be included in the phytoplankton group.

2.5 Chlorophyll concentration

Chlorophyll concentrations were measured on extracts from filtered samples via HPLC ([Chl]$_{HPLC}$, mg m^{-3}) performed by Horn Point Laboratory analytical services (University of Maryland Center for Environmental Science) using the method of Van Heukelem and Thomas (2001). Additionally, [Chl] was estimated using two methods. The first method was described above using the partitioning of the particulate absorption from the ac-s and ac-9 data.

For the second method, following Zhang et al. (2012), [Chl] was estimated from the VSF-inversion results based on the observed relationship between chlorophyll mass per cell ([Chl]$_{cell}$, g cell^{-1}) and mean cell size (radius) as illustrated in Fig. 2. Compared to Fig. 5 in Zhang et al. (2012), which used data from three studies (Stramski et al., 2001; Taguchi, 1976; Fujiki and Taguchi, 2002), Fig. 2 included data from five additional laboratory experiments reported in (Haardt and Maske, 1987; Morel and Bricaud, 1981; Privoznik et al.,
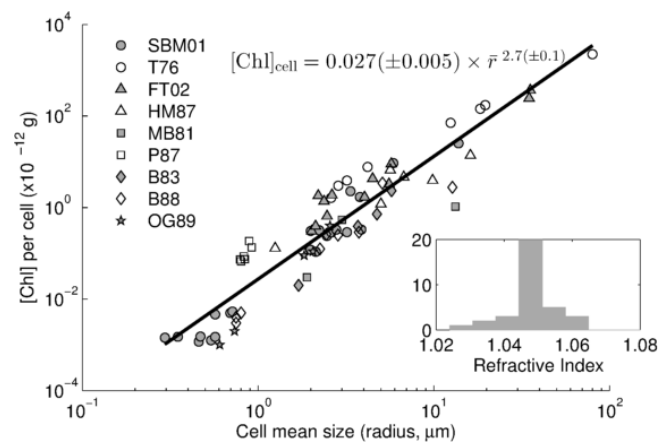
Fig. 2. The relationship between the chlorophyll mass per cell ([Chl]$_{cell}$, 10^{-12} g) as a function of cell mean size ($\bar{r}$, μm) was evaluated from laboratory measurements on different phytoplankton species from Stramski et al. (2001) (SBM01), Taguchi (1976) (T76), Fujiki and Taguchi (2002) (FT02), Haardt and Maske (1987) (HM87), Morel and Bricaud (1981) (MB81), Privoznik et al. (1978) (P87), Bricaud et al. (1983) (B83), Bricaud et al. (1988) (B88), and Osborne and Geider (1989) (OG89). The inset shows the distribution of the refractive index for phytoplankton species measured in SBM01 and B88.

1978; Bricaud et al., 1983, 1988; Osborne and Geider, 1989). The [Chl]$_{VSF}$ was estimated as,

$$[\text{Chl}]_{VSF} = \sum_i N_i \times 0.027 \times \bar{r}_i^{2.7}, \qquad (2)$$

using the relationship obtained in Fig. 2, and where N_i and $\bar{r}_i$ are respectively the concentration (cell m^{-3}) and the mean radius of subpopulation i whose refractive index is within the range of 1.03 to 1.08 and the mean radius is between 0.2 to $100\,\mu\text{m}$.

3 Results and discussion

3.1 Instrumental closure

Since both the ac-s and the MVSM-LISST allow the measurement of $b_{nw}(532)$, these two datasets were compared for instrumental closure (Zaneveld, 1994). From the ac-s data, the non-water scattering coefficient was first obtained as $b'_{nw}(532) = c'_{nw}(532) - a'_{nw}(532)$. From the MVSM-LISST VSFs, $b_{nw}(532) = 2\pi \int_{\theta_{min}}^{\theta_{max}} \beta_{nw}(532, \theta) \sin\theta\,d\theta$, where $\theta_{min} = 0.07°$ and $\theta_{max} = 179°$ are the minimum and maximum angles at which the VSF was measured. Note that $b_{nw}(532)$ estimated from the measured VSFs underestimated the true particulate scattering coefficient, for which θ_{min} should be $0°$ and θ_{max} should be $180°$. However, we did not estimate the total scattering coefficient by extending the measured VSFs into the extremities for two reasons. First, the scattering at angles less than $0.1°$ is increasingly
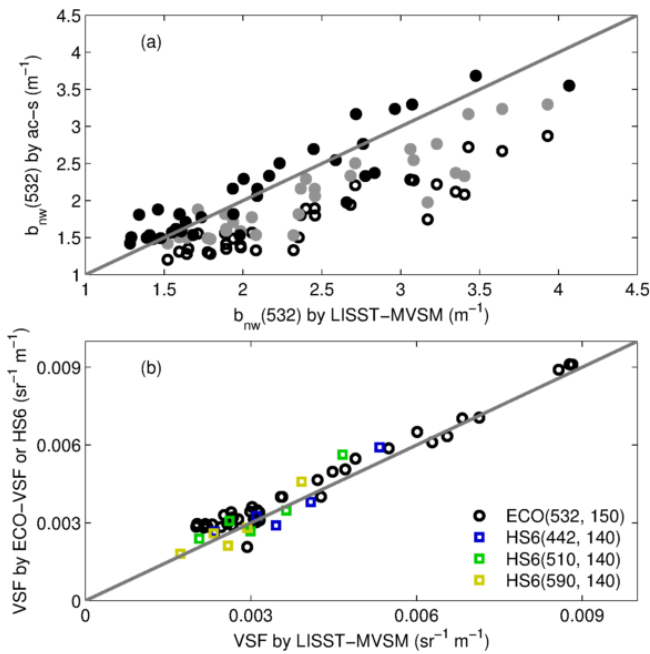
Fig. 3. Intercomparison between different instruments measuring scattering properties. **(a)** The comparisons of $b_{nw}(532)$ estimated from the ac-s and LISST-MVSM. Two scattering corrections were progressively applied to (1) $a_{nw}(532)$ to correct for scattering at angles from 41° to 180° that ac-s a-meter could not measure and (2) the LISST-MVSM based $b_{nw}(532)$ with integration only down to 0.93° to match the acceptance angle of ac-s c-meter. Open circles: neither correction was applied; grey circles: the 1st correction; black circles: both corrections. **(b)** The comparison of the LISST-MVSM $\beta(\lambda, \theta)$ with ECO-VSF data measured at 150° at 532 nm and with HydroScat-6 at 140° for three wavelengths of 442, 510 and 590 nm. For comparison with HydroScat-6 data, the spectral VSF values at the corresponding wavelengths were used.

affected, and sometimes dominated, by turbulence due to small scale temperature and salinity fluctuations (Bogucki et al., 1998). Second, because the VSF is weighted by a sine function of the scattering angle during the computation of b_{nw}, the error associated with this omission is small, often less than the instrument uncertainty. For example, the underestimation ranged from 1 % if the VSFs were assumed to be flat at the missing forward angles (a typical behavior based on Mie predictions) to 2 % if the VSFs were assumed to increase following a power law (to approximate the influence of turbulence; Bogucki et al., 1998). For comparison, the measurement uncertainty for the ac-s is $\sim 0.005\,\mathrm{m}^{-1}$ (Twardowski et al., 1999), or about 0.2 to 0.5 % in our case, ~ 6 % for the LISST (Slade and Boss, 2006), and ~ 5 % for the MVSM (Berthon et al., 2007).

As shown in Fig. 3a (open circles), the two datasets are highly correlated (Pearson correlation coefficient $r = 0.93$). However, the values of $b'_{nw}(532)$ obtained from the ac-s are systematically less than those from the VSFs by an average of 27 % (mean percentage difference, MPD), which is greater than the inherent instrument uncertainties. This underestimation of the scattering coefficient by the ac-s is expected (McKee et al., 2008; Leymarie et al., 2010) for two reasons: (1) the effect of the acceptance angle of an ac-s, which, at about 0.9°, is more than ten times larger than the θ_{min} used in estimating b_{nw} from the VSF; and (2) the ac-s a-meter cannot measure scattering at angles larger than $\sim 41°$ (the critical angle for total internal reflection for the submerged flow tube). Using Monte Carlo simulations based on Fournier and Forand particle phase functions (Fournier and Forand, 1994), McKee et al. (2008) estimate that these effects, if uncorrected, could lead to underestimates of ~ 67 % or more in b_{nw}. These are about twice as large as the error we observed in Fig. 3a, probably because of the significant differences between the Fournier and Forand phase functions used in the simulation and the VSFs we measured (results not shown). To further evaluate the effect of scattering on a-meter and c-meter measurements, we progressively applied two corrections: (1) the proportional scattering error correction was applied to a'_{nw} following Zaneveld et al. (1994) with 715 nm as the reference wavelength, and 2) setting θ_{min} to 0.93° while computing b_{nw} from the VSF to correct for the effect of the c-meter acceptance angle (Boss et al., 2009). Applying the first correction (grey circles in Fig. 3a), as is typically done with ac-s data, reduced the MPD by nearly 50 %. Applying both corrections (black circles in Fig. 3a) significantly improved the comparison by decreasing the MPD to 3 %, which is well within the instrument uncertainty range. Since the 1st correction is routinely applied to the ac measurements, we estimated that the typical ac-s estimates of the scattering coefficient (grey circles in Fig. 3a) would have to be multiplied by ~ 1.20 to match the estimates based on the extended angular measurement of the VSF.

The VSF measurements by the ECO-VSF (150° at 532 nm) and the Hydroscat-6 (140° at 442, 510 and 590 nm) were compared with the LISST-MVSM (Fig. 3b). The measurements from the three instruments were highly correlated ($r = 0.94$ or better) and agreed with each other within 5 %.

Only a few studies have been conducted to evaluate the optical closure of IOPs or to compare results from different instruments (Pegau et al., 1995; Kirk and Oliver, 1995; Chang and Whitmire, 2009; Whitmire et al., 2010; Twardowski et al., 2007; Boss et al., 2004). For example, Pegau et al. (1995) found that estimates of the scattering coefficient at Lake Pend Oreille, Idaho, from an ac-9 meter and from Petzold's (Petzold, 1972) General Angle Scattering Meter (GASM) did not agree with each other consistently. They attributed this intermittent lack of closure to the method for determining the scattering coefficient for the GASM, which only measures scattering from 10 to 170°. On the other

hand, Boss et al. (2004) show that the backscattering ratio estimated from the VSFs measured by the ECO-VSF, HS6 and Volume Scattering Meter (Lee and Lewis, 2003) (a prior version of the MVSM) agreed with each other to within 10 % for coastal waters off New Jersey. Compared with these previous results and considering the inherent instrument uncertainties, we feel that the level of agreement achieved in the present study is acceptable and indicates inter-instrument consistency of the measurements. In the highly spatially and temporally variable coastal waters that we sampled, the scatter in the data would certainly have been reduced if the instruments were deployed in the same package. Hereafter, for our measurements of scattering and backscattering, we will use $b_{nw}(532) = 2\pi \int_{\theta_{min}}^{\theta_{max}} \beta_{nw}(532, \theta) \sin\theta \, d\theta$, where $\theta_{min} = 0.07°$ and $\theta_{max} = 179°$, and $b_{bnw}(532) = 2\pi \int_{90}^{\theta_{max}} \beta_{nw}(532, \theta) \sin\theta \, d\theta$.

3.2 VSF-inversion results

Two examples of the outputs from the inversion are shown in Fig. 4 for station CB3: (1) on 20 October 2009, one day after a week-long heavy precipitation event over the area, and (2) on 22 October 2009, when an algal bloom was observed with more than a 2-fold increase in [Chl]$_{HPLC}$. The modeled VSF very closely matches the measured VSF (Fig. 4a and c). Comparing the total particle size distributions (PSD), obtained by summing all particle populations, with those from the LISST measurements over the overlapping size range (Fig. 4b and d) indicates that the PSDs from the two scattering-based methods agreed very well. An in-depth comparison for coastal areas in the US showed that the overall agreement of the PSDs between the VSF-inversion and LISST is within 10 % (Zhang et al., 2012). During the bloom, when [Chl] more than doubled, the concentration of phytoplankton particles increased by more than two orders of magnitude. This occurred mostly by the addition of smaller cells to those already present, and was accompanied by a twenty-fold increase in VSP, while there was relatively little change in the NAP concentration. Also, phytoplankton particles became the dominant particle type in the size range from 0.8 to 2 µm during the bloom. As a result, the angular scattering in the backward directions due to phytoplankton particles increased (the green curve in Fig. 4c vs. Fig. 4a), although their overall contribution to the backscattering remained small.

The retrieved average fractional contributions (±one standard deviation) by the three particle groups to the bulk VSFs and PSDs for all VSFs measured are shown in Fig. 5. In the forward directions, the VSF is strongly dominated by NAP scattering, while VSP accounted for most of the observed backscattering (Fig. 5a). For the PSD (Fig. 5b), on average, over 80 % of non-VSP particles are NAP, even though, occasionally (e.g., during the bloom), the retrieved abundance of phytoplankton particles exceeded NAP within certain size ranges (also see Fig. 4). Chesapeake Bay has a di-
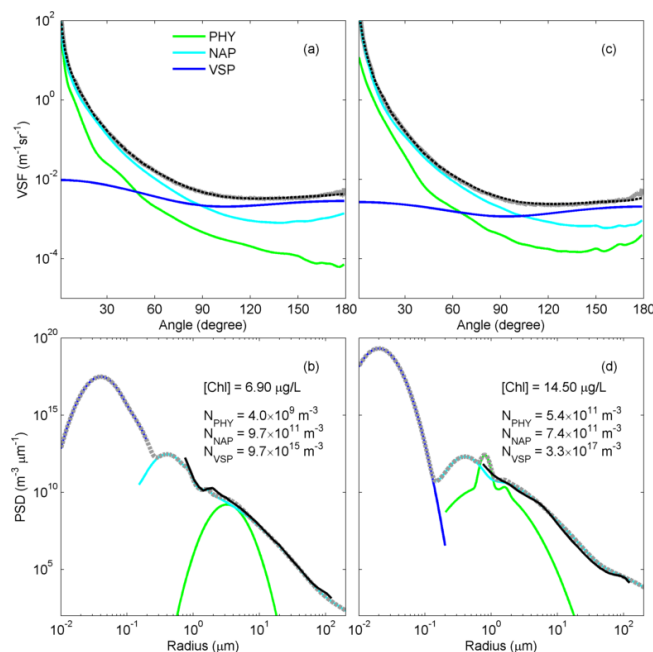

Fig. 4. Inversion results for station CB3 (circled in Fig. 1) on 20 October 2009, (**a** and **b**), one day after an extended rain event and on 22 October (**c** and **d**) when an algal bloom was observed. (**a** and **c**) The measured VSFs were partitioned into contributions by phytoplankton particles (PHY), non-algal particles (NAP) and very small particles (VSP). The solid gray lines are the measured VSFs and the dashed black lines are the sum of the groups' VSFs representing the best fit obtained during the inversion. (**b** and **d**) The corresponding particle size distributions (PSD) for the three particle groups (cut off at the filter pore size of ~ 0.2 µm). The solid black lines are the PSDs derived from the LISST measurements and the dashed gray lines are the sum of the PSDs for each group. Also shown are the HPLC chlorophyll concentration ([Chl] on the figure) and the particle concentration estimated for each group.

verse assemblage of phytoplankton species dominated by diatoms throughout the year with large seasonal fluctuations of chlorophytes, cyanobacteria, cryptophytes and dinoflagellates (Marshall et al., 2005). From Fig. 5, it appears that phytoplankton were not the dominant particle type, either numerically or in terms of their contribution to scattering, in Chesapeake Bay during the experiment. Yet, this non-dominant population could be identified and quantified through the VSF-inversion, mainly because phytoplankton particles exhibit an angular scattering signature that is distinct from other particles (e.g., Fig. 4a and c).

Figure 6 presents the variations of the measured bulk b_{nw}, b_{bnw} and $\tilde{b}_{bnw}$ ($= b_{bnw}/b_{nw}$) as well as the estimated b_{nw}, b_{bnw} and $\tilde{b}_{bnw}$ of individual components retrieved from the inversion as a function of [Chl]$_{HPLC}$; Table 1 shows the correlation coefficients between these variables and others used in this study. Contrary to the typical behavior observed in Case 1 waters (Dall'Olmo et al., 2009; Antoine et al., 2011;

Table 1. Pearson correlation coefficient (r) matrix for parameters that are either directly measured or derived from the inversion. S represents salinity. The values in bold face indicate that the correlations are statistically significant ($p < 0.05$). The scattering variables (b_{nw} and b_{bnw}, and their components of PHY, NAP and VSP) are measured and estimated at 532 nm. The absorption coefficients for CDOM and NAP are estimated at 412 nm. The [Chl] is measured using HPLC.
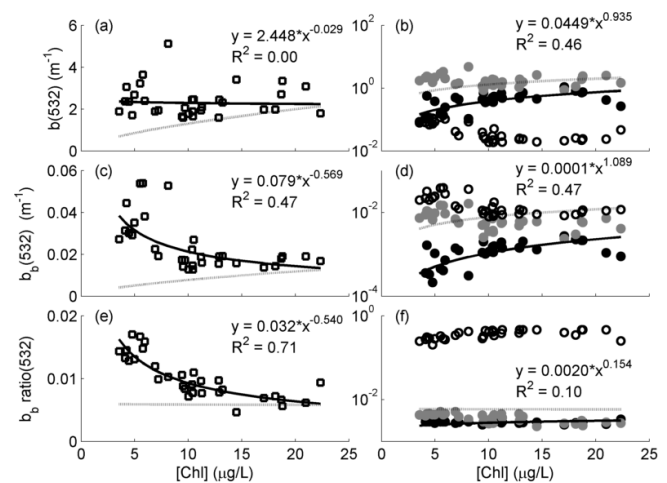
	[Chl]	b_{nw}	b_{PHY}	b_{NAP}	b_{VSP}	b_{bnw}	b_{bPHY}	b_{bNAP}	b_{bVSP}	a_{CDOM}	a_{NAP}
S	−0.20	**−0.43**	**0.33**	**−0.48**	**−0.43**	**−0.52**	**0.33**	**−0.52**	**−0.52**	**−0.83**	**−0.64**
[Chl]		−0.02	**0.59**	−0.20	**−0.66**	**−0.58**	**0.61**	**−0.51**	**−0.61**	−0.11	**−0.44**
b_{nw}			−0.22	**0.97**	**0.35**	**0.69**	−0.21	**0.80**	**0.63**	**0.55**	**0.79**
b_{PHY}				**−0.45**	**−0.53**	**−0.44**	**0.99**	**−0.50**	**−0.47**	**−0.33**	−0.26
b_{NAP}					**0.46**	**0.75**	**−0.45**	**0.87**	**0.71**	**0.59**	**0.80**
b_{VSP}						**0.88**	**−0.55**	**0.76**	**0.92**	**0.48**	**0.59**
b_{bnw}							**−0.45**	**0.96**	**0.99**	**0.59**	**0.83**
b_{bPHY}								**−0.50**	**−0.48**	**−0.33**	−0.25
b_{bNAP}									**0.93**	**0.58**	**0.84**
b_{bVSP}										**0.59**	**0.80**
a_{CDOM}											**0.68**
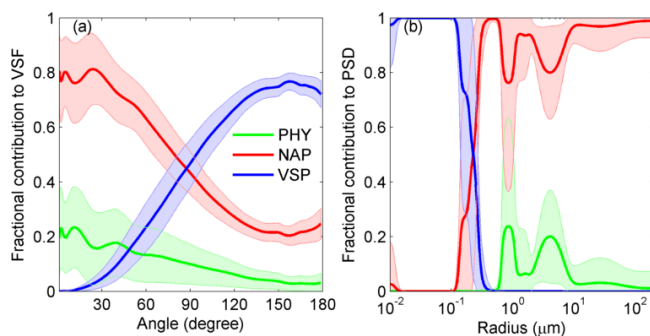
Fig. 5. Average fractional contributions by each of the three particle groups to **(a)** the VSF and **(b)** the PSD. The shaded areas represent one standard deviation.

Fig. 6. Relationships of [Chl]$_{HPLC}$ with the scattering coefficient (**a** and **b**), the backscattering coefficient (**c** and **d**), and the backscattering ratio (**e** and **f**). Open squares (left column) are the bulk parameters estimated directly from the measured VSFs. Open circles, grey circles and black circles (right column) are the variables for the particle groups of VSP, NAP and PHY, derived from the VSF-inversion. The dotted gray line in each panel represents the corresponding open ocean water model from Huot et al. (2008). The solid line in each panel represents a power-law regression against [Chl]$_{HPLC}$ of b_{nw}(532), b_{bnw}(532) or $\tilde{b}_{bnw}$(532) in (**a**), (**c**) and (**e**) respectively or of b_{PHY}(532), b_{bPHY}(532) or $\tilde{b}_{bPHY}$(532) in (**b**), (**d**) and (**f**) respectively. The equation of this power-law regression and the corresponding coefficient of determination (R^2) are also shown in each panel.

Huot et al., 2008) and in other coastal waters (Sullivan et al., 2005), b_{bnw} was found to decrease with [Chl]$_{HPLC}$ (Fig. 6c) while b_{nw} and [Chl]$_{HPLC}$ were not correlated ($R^2 = 0.00$, Fig. 6a). As expected from Fig. 6a and c, the backscattering ratio showed significant negative covariation with [Chl]$_{HPLC}$ (Fig. 6e). All relationships empirically derived between b_{nw}, b_{bnw}, $\tilde{b}_{bnw}$ and [Chl]$_{HPLC}$ (the solid curves in Fig. 6a, c and e) are, as expected, well above published Case 1 water relationships (Huot et al., 2008). This is consistent with a greater contribution from VSP and NAP compared with open ocean waters. It is also interesting to note that, as [Chl] increases, all bulk scattering parameters (b_{nw}, b_{bnw} and $\tilde{b}_{bnw}$) approach the Case 1 water relationships; this suggests an influence of phytoplankton and associated particles on the b_{nw} and b_{bnw} that approaches that for open ocean waters.

We examined these relationships more closely using the inverted contribution from the three particle groups (Fig. 6b, d and f). The first and most obvious observation (Fig. 6b) is that the VSPs contribute very little to the total scattering, which is dominated by the forward angles (also see

Figs. 4 and 5); the majority of the scattering originates from the NAP. Phytoplankton account for most of the remaining scattering for [Chl]$_{HPLC}$ above ~ 7 mg m^{-3} while below this concentration the impact of VSPs is closer to that of phytoplankton, but both contributions are only about 10–20 % of NAP. The impact of VSPs is, however, much different

in the case of backscattering (Fig. 6d). The VSPs dominate backscattering and the contribution of NAPs is lower by a factor of 2 to 3. Phytoplankton particles are the only ones for which the scattering and backscattering increase with chlorophyll concentration ($r = 0.59$ and 0.61 for b_{PHY} and b_{bPHY} vs. $[Chl]_{HPLC}$ respectively, Table 1), but they never make up more than 20 % of the total scattering or 10 % of the total backscattering. Previous measurements of $\tilde{b}_{bnw}$ in Case 1 waters have values between ~ 0.005 and 0.013 (Huot et al., 2008; Antoine et al., 2011; Whitmire et al., 2010) that show no or very little dependence on the trophic level (but see Twardowski et al., 2001) while coastal waters span a much greater range as observed here (also see Twardowski et al., 2001). The particles used for the inversion have a backscattering ratio of between 0.002 and 0.005 for NAP and between 0.0007 and 0.0034 for phytoplankton while the VSPs have a backscattering ratio of 0.2 to 0.45. Therefore, the rapid decrease in the backscattering ratio observed in our study must originate mostly from the decreasing contribution of VSPs with increasing chlorophyll concentration. Indeed, Table 1 shows that b_{VSP} or b_{bVSP} had the most negative correlation with $[Chl]_{HPLC}$.

Notably, while b_{nw} and b_{bnw} at high $[Chl]_{HPLC}$ are near the Case 1 water relationships, the phytoplankton fraction of backscattering (b_{bPHY}), even in these high $[Chl]$ waters, is well below that of the "high" chlorophyll Case 1 water relationship. This suggests that even in high chlorophyll Case 1 waters, a significant portion of the backscattering originates from the phytoplankton-associated NAP particles. It has been acknowledged that the homogeneous spherical assumption of the Mie theory is a major uncertainty in estimating the backscattering efficiency of oceanic particles, including phytoplankton (Stramski et al., 2004; Clavano et al., 2007). To overcome the uncertainty associated with the spherical assumption, we used an asymmetric hexahedral shape which was shown to appropriately simulate the scattering by mineral aerosol particles that do not possess a particular shape (Bi et al., 2010). For phytoplankton particles with the same refractive index and size distribution, using a hexahedral shape generally results in an average 2–3 fold increase in the backscattering ratio. Even with this increased backscattering efficiency, our inversion results showed that the phytoplankton contribution represents 10–70 % of scattering and 3–30 % of backscattering of the Huot et al. (2008) relationships (gray lines in Fig. 6), which is still consistent (or at least not contradictory) with the previous theoretical calculations based on the homogeneous spherical assumption (Morel and Ahn, 1991; Stramski and Kiefer, 1991). But there are still uncertainties associated with the homogeneous assumption of particles (e.g., Meyer, 1979).
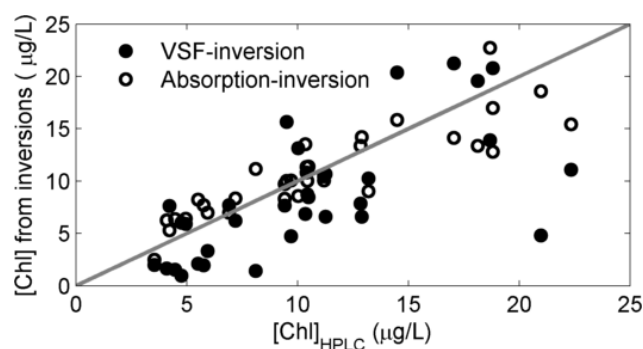

Fig. 7. Comparison of [Chl] estimated from the VSF-inversions (Eq. 2) and from the absorption spectrum inversion with the HPLC measurements.

3.3 Biogeochemical origins of scattering and absorbing particles

Generally speaking, scattering is mainly affected by the real part of the refractive index whereas absorption depends on the imaginary part, particularly for "soft" particles, such as those in the ocean (e.g., van de Hulst, 1981). For a given particle population, both vary with the number concentration and size distribution. Therefore, we should expect some consistency between the biogeochemical properties inverted from their respective measurements.

Estimates of [Chl] by the absorption- and the VSF-inversions compared well with $[Chl]_{HPLC}$ (Fig. 7) with $r = 0.68$ and MPD $= -20$ % for $[Chl]_{VSF}$ vs. $[Chl]_{HPLC}$ and $r = 0.80$ and MPD $= 9$ % for $[Chl]_{ac-s}$ vs. $[Chl]_{HPLC}$. The general agreement for [Chl] estimated by different methods also supports the validity of the VSF- and the absorption-inversions.

While [Chl] is frequently measured based on the absorption of photons by photosynthetic pigments and their subsequent emission through fluorescence, estimates of [Chl] from VSF-inversion has only recently been attempted (Zhang et al., 2012). It relies on (1) the allometric relationship between [Chl] per cell and cell sizes (Fig. 2), and (2) the retrieval of PSDs of phytoplankton cells. The agreement for the [Chl] estimates shown in Fig. 7 indicates that we were able to identify the signature of the chlorophyll-containing phytoplankton cells in both the scattering and absorption measurements and obtain quantitative estimates of [Chl] (with an uncertainty of approximately 20 %). Of particular significance is that the estimates of $[Chl]_{VSF}$ were obtained in an environment where phytoplankton, despite their high concentration, generally accounted for less than 20 % of scattering in both the forward and backward directions (Figs. 5 and 6) and where b_{nw} and b_{bnw} were not positively correlated with [Chl]. The latter point is significant since it means that a subpopulation was identified that was not correlated or that was inversely correlated with the total particulate scattering and backscattering (see Table 1). Since the scattering-based

approach was not sensitive to the chlorophyll molecules per se (they form only a small fraction of the total mass) but to the scattering from the whole cell, predominantly composed of carbon, the variable carbon to chlorophyll ratio of the cell will add further noise to the relationships. Estimates of phytoplankton biomass, that is the concentration of carbon associated with phytoplankton, would thus probably be better estimated by the VSF inversion. For example, Martinez-Vicente et al. (2013) found a significant relationship between $b_{bnw}(470)$ and the phytoplankton carbon concentration for Atlantic Ocean waters with [Chl] less than $0.4 \, \mathrm{mg \, m^{-3}}$. It will, thus, be of interest to continue evaluating the performance of the VSF-inversion technique to verify estimates of cell numbers or carbon concentration (the latter remains difficult to measure in the ocean). Furthermore, at this point, we have not examined if the subpopulations identified by this inversion are associated with specific algal groups. As such, we cautiously prefer to interpret these distributions as providing an overall representation of the whole phytoplankton community. Further work will examine if specific phytoplankton groups can be distinguished.

We now turn to the remaining two particle groups. The VSF-inversion distinguishes different particle populations based on the phase functions, which are not very sensitive to absorption (or the imaginary part of the refractive index) (Zhang et al., 2011). Therefore, it is challenging to derive the absorption properties from the VSF-inversion and to compare directly with absorption-based estimates. Instead, we examined the covariability between the scattering and the absorption of the two particles groups (Fig. 8).

For the VSF-inversion, the VSP group, representing those subpopulations with a mode radius less than $0.1 \, \mu m$, corresponds roughly to dissolved (based on filtration with a pore size of $0.2 \, \mu m$) particles of sizes (in radius) from 0.01 to $0.1 \, \mu m$ (see Fig. 5b). It should also be noted that for VSPs, the phase functions vary much more strongly with the size distribution than the refractive index (Zhang et al., 2011); therefore, it is difficult to further differentiate VSPs into, say, organic or inorganic fractions, from the VSF-inversion. On the other hand, CDOM estimates based on filtration represent the colored portion of particles and complex molecules with sizes less than the pore size of the filter used. Figure 8a compares VSF-inversion derived $b_{bVSP}(532)$ and $a_{CDOM}(412)$ measured using the ac-9 inline with a $0.2 \, \mu m$ filter. The scatter between $b_{bVSP}(532)$ and $a_{CDOM}(412)$ shown in Fig. 8c is expected because of the differences in the two populations that these two parameters represent and the differences between the optical processes underlying scattering and absorption. Despite these differences, the two variables do correlate with each other significantly ($r = 0.59$, Table 1). Also, both varied inversely with salinity (Table 1), possibly indicating a common source of origin in riverine runoff. While circumstantial, these factors suggest that there might be a significant overlap between the two particle populations represented by $b_{bVSP}(532)$ and $a_{CDOM}(412)$, respectively. For example, it
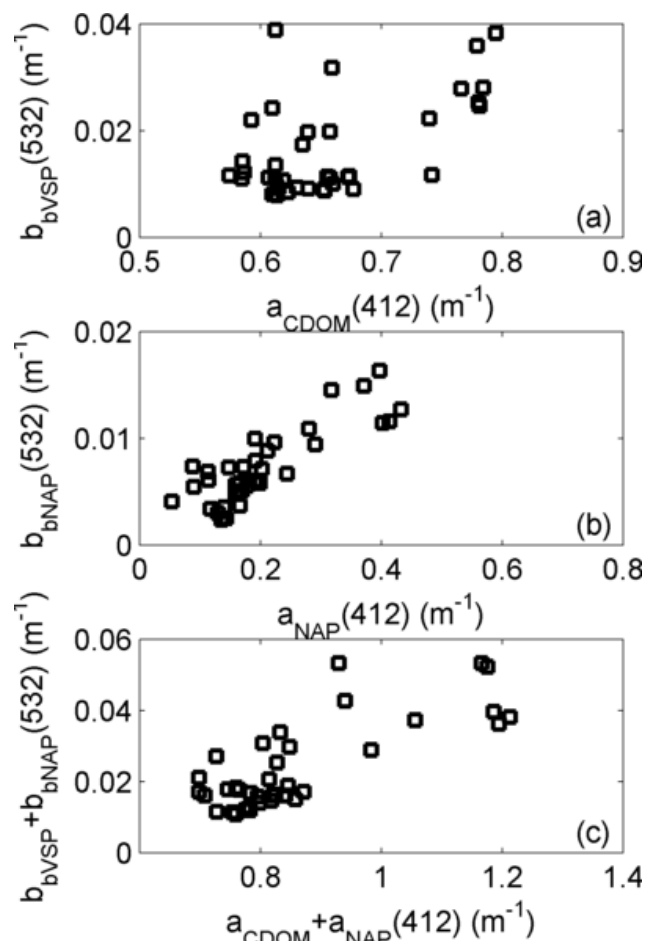
Fig. 8. Intercomparisons of measured absorption and estimated backscattering coefficients for CDOM and NAP. **(a)** $a_{CDOM}(412)$ measured using the ac-9 with a 0.2-μm filter vs. $b_{bVSP}(532)$ estimated for the VSP group from the VSF-inversion. **(b)** $a_{NAP}(412)$ estimated from the ac-s absorption inversion vs. $b_{bNAP}(532)$ estimated for the NAP group from the VSF-inversion. **(c)** absorption coefficient for the NAM population, $a_{CDOM}(412) + a_{NAP}(412)$ vs. the backscattering scattering coefficient for the NAM population, $b_{bVSP}(532) + b_{bNAP}(532)$.

can be expected that filtrate contains small particles that both absorb and scatter light. This also implies that CDOM defined based on filtration does scatter light, particularly in the backward direction (also see Fig. 5).

The NAP derived from the VSF-inversion is defined as populations that are relatively large (i.e., not VSP) and whose refractive index *is not* in the range of 1.03 to 1.08 (i.e., not phytoplankton). The NAP derived from absorption-inversion is based on the assumed power-law spectral shape (see Eq. 1) using the absorption spectra with the CDOM contribution removed. Table 1 shows that among the variables derived from the VSF-inversion, $a_{NAP}(412)$ correlates best with $b_{bNAP}(532)$ ($\rho = 0.84$) and $b_{NAP}(532)$ ($\rho = 0.80$). The correlations of $b_{bNAP}(532)$ and $b_{NAP}(532)$ with $a_{NAP}(412)$

are also slightly higher (though not significantly different) than $b_{bnw}(532)$ and $b_{nw}(532)$. A detailed comparison of $a_{NAP}(412)$ and $b_{bNAP}(532)$ is shown in Fig. 8b. As we acknowledged before, the partition for NAP from the VSF-inversion is not exclusive, and it is very likely that natural NAP particles could have an index of refraction in the range of 1.03–1.08. To account for the non-sphericity of natural particles, we have assumed that all particles have a hexahedral shape. The shape effect, while negligible for small particles (e.g., VSP), could be significant for larger particles (NAP or PHY) (Mishchenko et al., 2006; Clavano et al., 2007). In spite of these uncertainties, Fig. 8 does indicate a certain level convergence for NAP from both the scattering and absorption perspectives. A similar observation was made by Chami et al. (2006) who found that $\beta_{nw}(443, 140°)$, while having no correlation with phytoplankton absorption, correlated significantly with $a_{NAP}(400)$ in a coastal environment in the Black Sea. They further concluded that the same particles contributing to a_{NAP} were also the major contributors to $\beta_{nw}(443, 140°)$. But, in this study, we were able to further quantify the scattering caused only by NAP.

Since samples passing through the 0.2 μm filter are essentially devoid of chlorophyll-bearing particles (Chavez et al., 1995), the major difference between the dissolved and NAP fractions is the particle size. Indeed, Table 1 shows that the optical properties, either measured or derived for these two general particle fractions, covary significantly (e.g., $r = 0.80$ for $a_{NAP}(412)$ vs. $b_{bVSP}(532)$ and $r = 0.68$ for $a_{CDOM}(412)$ vs. $a_{NAP}(412)$) and all vary inversely with salinity. If we ignore the operational definition of dissolved particles for the moment (see e.g., Stramski et al., 2004), then the combined dissolved and NAP fractions would represent the total non-algal matter (NAM). One advantage of examining this NAM is that the possible optical effect due to the artificial size partition is reduced. Figure 8c, comparing $a_{CDOM}(412) + a_{NAP}(412)$ and $b_{bVSP}(532) + b_{bNAP}(532)$, shows that the two NAM populations based on the VSF- and the absorption-inversions are highly related ($r = 0.79$), either representing the same particle population or two closely correlated populations. This also explains the existence of general covariability in the optical properties between these two populations.

4 Conclusions

IOPs provide the fundamental linkage between biogeochemical and optical properties of particle populations. In this contribution, we have provided the first experimental evidence that it is possible to invert the VSF to obtain the abundance of "dissolved" matter (VSP and/or CDOM), non-algal particles and phytoplankton populations, which have been traditionally derived from spectral absorption. Indeed, all comparisons between the concentrations of dissolved matter, NAP and phytoplankton that have been made using absorption-

based methods and those made by inverting the VSF have showed that the estimates were well correlated. Furthermore, the VSF-inversion provided reasonably accurate measurements of [Chl] in the complex case 2 waters of Chesapeake Bay. Most notably, the potential for retrieving [Chl] using the VSF-based method was highlighted when both particulate scattering and backscattering showed, respectively, no correlation and a decreasing relationship with chlorophyll.

Particles, both small and large, scatter light. Even truly dissolved matter, such as sea salts, scatter light by modifying the density fluctuations of seawater (e.g., Zhang et al., 2009). This certainly applies to operationally-defined dissolved organic matter, including CDOM. However, bio-optical modeling often assumes that CDOM has no contribution to scattering (or backscattering) (e.g., Siegel et al., 2005; Lee et al., 2002). This may be the case for clear oceanic water where scattering by CDOM is negligible, but it is questionable for coastal and estuary environments. The VSF-inversion results indicated that while the scattering due to VSPs is typically negligible (at most 5 %) compared with larger particles, VSPs dominated backscattering (Fig. 6). We also found the VSP backscattering correlated significantly with the measured CDOM absorption. Both varied inversely with salinity, possibly indicating a common biogeochemical source contributing to both the inferred backscattering and the measured absorption by small (or dissolved) particles.

Presently, there is an ongoing debate concerning the "missing" backscattering source in the ocean (Stramski et al., 2004). With the limitation that the scattering efficiencies of the particle subpopulations used herein are based on theory, our results seem to support the earlier theoretical studies suggesting that small submicron particles are responsible for most of the non-water backscattering in the ocean (Stramski and Kiefer, 1991; Ulloa et al., 1994). This is also corroborated by simulations of colloidal particles using actual measurements of colloid concentrations and size distributions in seawater (Stramski and Wozniak, 2005). But recent field investigations in the open ocean suggest that larger particles may be more important in backscattering (Dall'Olmo et al., 2009; Westberry et al., 2010; Martinez-Vicente et al., 2013). Both theoretical and field investigations have inherent uncertainties. It is nearly impossible to single out a particular population even in laboratory settings (e.g., Whitmire et al., 2010), let alone in the field. On the other hand, theoretical simulations make unrealistic assumptions about particles. For example, the assumption of homogeneous spheres is known to lead to lowered estimates of backscattering than equivalent non-spherical (e.g., Clavano et al., 2007) or non-homogeneous particles (Kitchen and Zaneveld, 1992; Quirantes and Bernard, 2006; Zhang et al., 1998). In computing the kernel function for the VSF-inversion, particles are represented by homogeneous asymmetrical hexahedral. While an asymmetrical hexahedral is nearly an extreme morphological opposite to a sphere, the assumption of homogeneity might have led to

an underestimation of backscattering, particularly for relatively large (i.e., non-VSP) particles, which in turn may lead to an artificial elevation of the retrieved backscattering contribution by VSP particles. We do not know the uncertainty associated with this homogeneous particle assumption. However, our results have shown [Chl] estimated for phytoplankton particles, which are known to have a variety of internal and "shell" structure among different species, agreed well with the independent HPLC data. While uncertainty remains as to the sources of backscattering, we caution against the "convenient" assumption that CDOM does not scatter light, particularly in turbid coastal waters.

As can be expected for turbid environments such as the Chesapeake Bay, the phytoplankton population was not the dominant particle group either numerically or optically. The NAP population dominated the forward and the total scattering as well as the particle size distribution for sizes greater than $\sim 0.2 \, \mu m$ (Figs. 5 and 6). Both CDOM and NAP populations correlated significantly with the salinity (Table 1), possibly indicating a common origin from riverine runoff.

Because the VSF-inversion derives the size distribution and the refractive index simultaneously for individual particle populations, this approach holds great potential for identifying biogeochemical properties, particularly in combination with spectral measurements of absorption.

References

Aas, E.: Refractive index of phytoplankton derived from its metabolite composition, J. Plankton Res., 18, 2223–2249, doi:10.1093/plankt/18.12.2223, 1996.

Antoine, D., Siegel, D. A., Kostadinov, T., Maritorena, S., Nelson, N. B., Gentili, B., Vellucci, V., and Guillocheau, N.: Variability in optical particle backscattering in contrasting bio-optical oceanic regimes, Limnol. Oceanogr., 56, 955–973, 2011.

Babin, M. and Stramski, D.: Variations in the mass-specific absorption coefficient of mineral particles suspended in water, Limnol. Oceanogr., 49, 756–767, 2004.

Babin, M., Stramski, D., Ferrari, G. M., Claustre, H., Bricaud, A., Obolensky, G., and Hoepffner, N.: Variations in the light absorption coefficients of phytoplankton, nonalgal particles, and dis-

solved organic matter in coastal waters around Europe, J. Geophys. Res., 108, 3211, doi:10.1029/2001JC000882, 2003.

Berthon, J.-F., Shybanov, E., Lee, M. E. G., and Zibordi, G.: Measurements and modeling of the volume scattering function in the coastal northern Adriatic Sea, Appl. Optics, 46, 5189–5203, 2007.

Bi, L., Yang, P., Kattawar, G. W., and Kahn, R.: Modeling optical properties of mineral aerosol particles by using nonsymmetric hexahedra, Appl. Optics, 49, 334–342, 2010.

Bogucki, D. J., Domaradzki, J. A., Stramski, D., and Zaneveld, J. R. V.: Comparison of near-forward light scattering on oceanic turbulence and particles, Appl. Optics, 37, 4669–4677, 1998.

Boss, E., Pegau, W. S., Gardner, W. D., Zaneveld, J. R. V., Barnard, A. H., Twardowski, M. S., Chang, G. C., and Dickey, T. D.: Spectral particulate attenuation and particle size distribution in the bottom boundary layer of a continental shelf, J. Geophys. Res., 106, 9509–9516, doi:10.1029/2000jc900077, 2001.

Boss, E., Pegau, W. S., Lee, M., Twardowski, M., Shybanov, E., and Korotaev, G.: Particulate backscattering ratio at LEO 15 and its use to study particle composition and distribution, J. Geophys. Res., 109, C01014, doi:10.1029/2002JC001514, 2004.

Boss, E., Collier, R., Larson, G., Fennel, K., and Pegau, W. S.: Measurements of spectral optical properties and their relation to biogeochemical variables and processes in Crater Lake, Crater Lake National Park, OR, Hydrobiologia, 574, 149–159, 2007.

Boss, E., Slade, W. H., Behrenfeld, M., and Dall'Olmo, G.: Acceptance angle effects on the beam attenuation in the ocean, Opt. Express, 17, 1535–1550, 2009.

Bricaud, A., Morel, A., and Prieur, L.: Optical efficiency factors of some phytoplankters, Limnol. Oceanogr., 28, 816–832, 1983.

Bricaud, A., Bédhomme, A.-L., and Morel, A.: Optical properties of diverse phytoplanktonic species: experimental results and theoretical interpretation, J. Plankton Res., 10, 851–873, 1988.

Bricaud, A., Morel, A., Babin, M., Allali, K., and Claustre, H.: Variations of light absorption by suspended particles with chlorophyll *a* concentration in oceanic (case 1) waters: Analysis and implication for bio-optical models, J. Geophys. Res., 103, 31033–31044, 1998.

Campbell, J. W.: The lognormal distribution as a model for bio-optical variability in the sea, J. Geophys. Res., 100, 13237–13254, 1995.

Carder, K., Betzer, P., and Eggimann, D.: Physical, Chemical, and Optical Measures of Suspended-Particle Concentrations: Their Intercomparison and Application to the West African Shelf, in: Suspended Solids in Water, edited by: Gibbs, R., Marine Science, Springer US, 173–193, 1974.

Chami, M., Shybanov, E. B., Churilova, T. Y., Khomenko, G. A., Lee, M. E. G., Martynov, O. V., Berseneva, G. A., and Korotaev, G. K.: Optical properties of the particles in the Crimea coastal waters (Black Sea), J. Geophys. Res., 110, C11020, doi:10.1029/2005jc003008, 2005.

Chami, M., Shybanov, E. B., Khomenko, G. A., Lee, M. E.-G., Martynov, O. V., and Korotaev, G. K.: Spectral variation of the volume scattering function measured over the full range of scattering angles in a coastal environment, Appl. Optics, 45, 3605–3619, 2006.

Chang, G. and Whitmire, A. L.: Effects of bulk particle characteristics on backscattering and optical closure, Opt. Express, 17, 2132–2142, 2009.

Chavez, F. P., Buck, K. R., Bidigare, R. R., Karl, D. M., Hebel, D., Latasa, M., Campbell, L., and Newton, J.: On the chlorophyll *a* retention properties of glass-fiber GF/F filters, Limnol. Oceanogr., 40, 428–433, 1995.

Chin, J. H., Sliepcevich, C. M., and Tribus, M.: Particle Size Distributions from Angular Variation of Intensity of Forward-Scattered Light at Very Small Angles, J. Phys. Chem., 59, 841–844, doi:10.1021/j150531a010, 1955.

Ciotti, A. M., Lewis, M. R., and Cullen, J. J.: Assessment of the relationships between dominant cell size in natural phytoplankton communities and the spectral shape of the absorption coefficient, Limnol. Oceanogr., 47, 404–417, 2002.

Clavano, W. R., Boss, E., and Karp-Boss, L.: Inherent Optical Properties of Non-Spherical Marine-Like Particles – From Theory to Observation, in: Oceanography and Marine Biology: An Annual Review, edited by: Gibson, R. N., Atkinson, R. J. A., and Gordon, J. D. M., Taylor & Francis, Boca Raton, 1–38, 2007.

Coston, S. D. and George, N.: Particle sizing by inversion of the optical transform pattern, Appl. Optics, 30, 4785–4794, 1991.

Czerski, H., Twardowski, M., Zhang, X., and Vagle, S.: Resolving size distributions of bubbles with radii less than 30 μm with optical and acoustical methods, J. Geophys. Res., 116, C00H11, doi:10.1029/2011jc007177, 2011.

Dall'Olmo, G., Westberry, T. K., Behrenfeld, M. J., Boss, E., and Slade, W. H.: Significant contribution of large particles to optical backscattering in the open ocean, Biogeosciences, 6, 947–967, doi:10.5194/bg-6-947-2009, 2009.

Doxaran, D., Babin, M., and Leymarie, E.: Near-infrared light scattering by particles in coastal waters, Opt. Express, 15, 12834–12849, 2007.

Doxaran, D., Ruddick, K., McKee, D., Gentili, B., Tailliez, D., Chami, M., and Babin, M.: Spectral variations of light scattering by marine particles in coastal waters, from visible to near infrared, Limnol. Oceanogr., 54, 1257–1271, 2009.

Estapa, M. L., Boss, E., Mayer, L. M., and Roesler, C. S.: Role of iron and organic carbon in mass-specific light absorption by particulate matter from Louisiana coastal waters, Limnol. Oceanogr., 57, 97–112, doi:10.4319/lo.2012.57.1.0097, 2012.

Fournier, G. R. and Forand, J. L.: Analytical phase function for ocean water, SPIE Ocean Optics XII, 2258, 194–201, 1994.

Fujiki, T. and Taguchi, S.: Variability in chlorophyll *a* specific absorption coefficient in marine phytoplankton as a function of cell size and irradiance, J. Plankton Res., 24, 859–874, doi:10.1093/plankt/24.9.859, 2002.

Gordon, H. R. and Brown, O. B.: A theoretical model of light scattering by Sargasso Sea particulates, Limnol. Oceanogr., 17, 826–832, 1972.

Gordon, H. R., Brown, O. B., Evans, R. H., Brown, J. W., Smith, R. C., Baker, K. S., and Clark, D. K.: A semianalytic radiance model of ocean color, J. Geophys. Res., 93, 10909–10924, 1988.

Gould, R. W., Arnone, J. R. A., and Martinolich, P. M.: Spectral dependence of the scattering coefficient in case 1 and case 2 waters, Appl. Optics, 38, 2377–2383, 1999.

Green, R. E., Sosik, H. M., Olson, R. J., and DuRand, M. D.: Flow cytometric determination of size and complex refractive index for marine particles: comparison with independent and bulk estimates, Appl. Optics, 42, 526–541, 2003.

Haardt, H. and Maske, H.: Specific in vivo absorption coefficient of chlorophyll *a* at 675 nm, Limnol. Oceanogr., 32, 608–619, 1987.

Huot, Y., Morel, A., Twardowski, M. S., Stramski, D., and Reynolds, R. A.: Particle optical backscattering along a chlorophyll gradient in the upper layer of the eastern South Pacific Ocean, Biogeosciences, 5, 495–507, doi:10.5194/bg-5-495-2008, 2008.

Kirk, J. T. O. and Oliver, R. L.: Optical closure in an ultraturbid lake, J. Geophys. Res., 100, 13221–13225, doi:10.1029/95jc00533, 1995.

Kitchen, J. C. and Zaneveld, J. R. V.: A three-layered sphere model of the optical properties of phytoplankton, Limnol. Oceanogr., 37, 1680-1690, 1992.

Knight, J. C., Ball, D., and Robertson, G. N.: Analytical inversion for laser diffraction spectrometry giving improved resolution and accuracy in size distribution, Appl. Optics, 30, 4795–4799, 1991.

Kullenberg, G.: Scattering of light by Sargasso Sea water, Deep-Sea Res., 15, 423–432, 1968.

Lambert, C. E., Jehanno, C., Silverberg, N., Brun-Cottan, J. C., and Chesselet, R.: Log-normal distribution of suspended particles in the open ocean, J. Mar. Res., 39, 77–98, 1981.

Lee, M. E. and Lewis, M. R.: A New Method for the Measurement of the Optical Volume Scattering Function in the Upper Ocean, J. Atmos. Ocean Tech., 20, 563–571, 2003.

Lee, Z., Carder, K. L., and Arnone, R. A.: Deriving inherent optical properties from water color: a multiband quasi-analytical algorithm for optically deep waters, Appl. Optics, 41, 5755–5772, 2002.

Leymarie, E., Doxaran, D., and Babin, M.: Uncertainties associated to measurements of inherent optical properties in natural waters, Appl. Optics, 49, 5415–5436, 2010.

Magnuson, A., Harding Jr., L. W., Mallonee, M. E., and Adolf, J. E.: Bio-optical model for Chesapeake Bay and the Middle Atlantic Bight, Estuar. Coast. Shelf. S., 61, 403–424, doi:10.1016/j.ecss.2004.06.020, 2004.

Marshall, H. G., Burchardt, L., and Lacouture, R.: A review of phytoplankton composition within Chesapeake Bay and its tidal estuaries, J. Plankton Res., 27, 1083–1102, 10.1093/plankt/fbi079, 2005.

Martinez-Vicente, V., Dall'Olmo, G., Tarran, G., Boss, E., and Sathyendranath, S.: Optical backscattering is correlated with phytoplankton carbon across the Atlantic Ocean, Geophys. Res. Lett., 40, 1–5, doi:10.1002/grl.50252, 2013.

McKee, D., Piskozub, J., and Brown, I.: Scattering error corrections for in situ absorption and attenuation measurements, Opt. Express, 16, 19480–19492, 2008.

Meyer, R. A.: Light scattering from biological cells: Dependence of backscattering radiation on membrane thickness and refractive index, Appl. Optics, 18, 585–588, 1979.

Mishchenko, M. I., Travis, L. D., and Lacis, A. A.: Multiple Scattering of Light by Particles: Radiative Transfer and Coherent Backscattering, Cambridge University Press, Cambridge, 478 pp., 2006.

Morel, A.: The scattering of light by seawater: experimental results and theoretical approach, NATO Advisory Group for Aerospace Research and Development, No. 61, 171, 1973.

Morel, A.: Optical modeling of the upper ocean in relation to its biogenous matter content (Case I waters), J. Geophys. Res., 93, 10749–10768, 1988.

Morel, A. and Ahn, Y.-H.: Optics of heterotrophic nanoflagellates and ciliates: A tentative assessment of their scattering role in

oceanic waters compared to those of bacterial and algal cells, J. Mar. Res., 49, 177–202, 1991.

Morel, A. and Bricaud, A.: Theoretical results concerning light absorption in a discrete medium and application to specific absorption of phytoplankton, Deep-Sea Res., 28, 1375–1393, 1981.

Morel, A. and Maritorena, S.: Bio-optical properties of oceanic waters: A reappraisal, J. Geophys. Res., 106, 7163–7180, 2001.

Morel, A. and Prieur, L.: Analysis of variations in ocean color, Limnol. Oceanogr., 22, 709–722, 1977.

Osborne, B. A. and Geider, R. J.: Problems in the assessment of the package effect in five small phytoplankters, Mar. Biol., 100, 151–159, 10.1007/bf00391954, 1989.

Pegau, W. S., Zaneveld, J. R. V., and Voss, K. J.: Toward closure of the inherent optical properties of natural waters, J. Geophys. Res., 100, 13193–13199, 1995.

Peng, F. and Effler, S. W.: Characterizations of individual suspended mineral particles in western Lake Erie: Implications for light scattering and water clarity, J. Great Lakes Res., 36, 686–698, doi:10.1016/j.jglr.2010.08.003, 2010.

Petzold, T. J.: Volume scattering function for selected ocean waters, Scripps Institute of Oceanography, La JollaSIO Ref. 72–78, 79, 1972.

Preisendorfer, R. W.: Hydrologic Optics: Introduction, Pacific Mar. Environ. lab/NOAA, Seattle, 218 pp., 1976.

Privoznik, K. G., Daniel, K. J., and Incropera, F. P.: Absorption, extinction and phase function measurements for algal suspensions of chlorella pyrenoidosa, J. Quant. Spectrosc. Ra., 20, 345–352, 1978.

Quirantes, A. and Bernard, S.: Light-scattering methods for modelling algal particles as a collection of coated and/or nonspherical scatterers, J. Quant. Spectrosc. Ra., 100, 315–324, doi:10.1016/j.jqsrt.2005.11.048, 2006.

Riley, J. B. and Agrawal, Y. C.: Sampling and inversion of data in diffraction particle sizing, Appl. Optics, 30, 4800–4817, 1991.

Sathyendranath, S., Prieur, L., and Morel, A.: A three-component model of ocean colour and its application to remote sensing of phytoplankton pigments in coastal waters, Int. J. Remote Sens., 10, 1373–1394, doi:10.1080/01431168908903974, 1989.

Siegel, D. A., Maritorena, S., Nelson, N. B., and Behrenfeld, M. J.: Independence and interdependencies among global ocean color properties: Reassessing the bio-optical assumption, J. Geophys. Res.-Oceans, 110, C07011, doi:10.1029/2004JC002527, 2005.

Slade, W. H. and Boss, E. S.: Calibrated near-forward volume scattering function obtained from the LISST particle sizer, Opt. Express, 14, 3602–3615, 2006.

Stramski, D. and Kiefer, D. A.: Light scattering by microorganisms in the open ocean, Prog. Oceanogr., 28, 343–383, 1991.

Stramski, D. and Wozniak, S. B.: On the role of colloidal particles in light scattering in the ocean, Limnol. Oceanogr., 50, 1581–1591, 2005.

Stramski, D., Bricaud, A., and Morel, A.: Modeling the inherent optical properties of the ocean based on the detailed composition of the planktonic community, Appl. Optics, 40, 2929–2945, 2001.

Stramski, D., Boss, E., Bogucki, D., and Voss, K. J.: The role of seawater constituents in light backscattering in the ocean, Prog. Oceanogr., 61, 27–56, 2004.

Sullivan, J. M., Twardowski, M. S., Donaghay, P. L., and Freeman, S. A.: Use of optical scattering to discriminate particle types in coastal waters, Appl. Optics, 44, 1667–1680, 2005.

Sullivan, J. M., Twardowski, M. S., Zaneveld, J. R. V., Moore, C. M., Barnard, A. H., Donaghay, P. L., and Rhoades, B.: Hyperspectral temperature and salt dependencies of absorption by water and heavy water in the 400–750 nm spectral range, Appl. Optics, 45, 5294–5309, 2006.

Sullivan, J. M. and Twardowski, M. S.: Angular shape of the oceanic particulate volume scattering function in the backward direction, Appl. Optics, 48, 6811–6819, 2009.

Taguchi, S.: Relationship between photosynthesis and cell size of marine diatom, J. Phycol., 12, 185–189, doi:10.1111/j.1529-8817.1976.tb00499.x, 1976.

Twardowski, M., Zhang, X., Vagle, S., Sullivan, J., Freeman, S., Czerski, H., You, Y., Bi, L., and Kattawar, G.: The optical volume scattering function in a surf zone inverted to derive sediment and bubble particle subpopulations, J. Geophys. Res., 117, C00H17, doi:10.1029/2011JC007347, 2012.

Twardowski, M. S., Sullivan, J. M., Donaghay, P. L., and Zaneveld, J. R. V.: Microscale Quantification of the Absorption by Dissolved and Particulate Material in Coastal Waters with an ac-9, J. Atmos. Ocean Tech., 16, 691–707, doi:10.1175/1520-0426(1999)016<0691:MQOTAB>2.0.CO;2, 1999.

Twardowski, M. S., Boss, E., Macdonald, J. B., Pegau, W. S., Barnard, A. H., and Zaneveld, J. R. V.: A model for estimating bulk refractive index from the optical backscattering ratio and the implications for understanding particle composition in case I and case II waters, J. Geophys. Res., 106, 14129–14142, 2001.

Twardowski, M. S., Claustre, H., Freeman, S. A., Stramski, D., and Huot, Y.: Optical backscattering properties of the "clearest" natural waters, Biogeosciences, 4, 1041–1058, doi:10.5194/bg-4-1041-2007, 2007.

Twomey, S.: Introduction to the mathematics of inversion in remote sensing and indirect measurements, Developments in Geomathematics, Elsevier Scientific Publishing Company, Amsterdam, 243 pp., 1977.

Ulloa, O., Sathyendranath, S., and Platt, T.: Effect of the particle-size distribution on the backscattering ratio in seawater, Appl. Optics, 33, 7070–7077, 1994.

Vaillancourt, R. D. and Balch, W. M.: Size distribution of marine submicron particles determined by flow field-flow fractionation, Limnol. Oceanogr., 45, 485–492, 2000.

van de Hulst, H. C.: Light Scattering by Small Particles, Dover Publications, Inc., New York, 1981.

Van Heukelem, L. and Thomas, C. S.: Computer-assisted high-performance liquid chromatography method development with applications to the isolation and analysis of phytoplankton pigments, J. Chromatogr. A, 910, 31–49, doi:10.1016/S0378-4347(00)00603-4, 2001.

Westberry, T. K., Dall'Olmo, G., Boss, E., Behrenfeld, M. J., and Moutin, T.: Coherence of particulate beam attenuation and backscattering coefficients in diverse open ocean environments, Opt. Express, 18, 15419–15425, 2010.

Whitmire, A. L., Pegau, W. S., Karp-Boss, L., Boss, E., and Cowles, T. J.: Spectral backscattering properties of marine phytoplankton cultures, Opt. Express, 18, 15073–15093, 2010.

Wozniak, B. and Dera, J.: Light Absorption in Sea Water, Atmospheric and Oceanographic Sciences Library, edited by: Mysak, L. A. and Hamilton, K., Springer, New York, 452 pp., 2007.

Yentsch, C. S.: Measurement of visible light absorption by particulate matter in the ocean, Limnol. Oceanogr., 7, 207–217, 1962.

Zaneveld, J. R. V.: Optical Closure: From theory to measurement, in: Ocean Optics, edited by: Spinrad, R. W., Carder, K. L., and Perry, M. J., Oxford University Press, New York, 59–73, 1994.

Zaneveld, J. R. V., Roach, D. M., and Pak, H.: The determination of the index of refraction distribution of oceanic particulates, J. Geophys. Res., 79, 4091–4095, 1974.

Zaneveld, J. R. V., Kitchen, J. C., and Moore, C.: The scattering error correction of reflecting-tube absorption meters, SPIE Ocean Optics XII, 2258, 44–55, 1994.

Zhang, X., Lewis, M. R., and Johnson, B. D.: Influence of bubbles on scattering of light in the ocean, Appl. Optics, 37, 6525–6536, 1998.

Zhang, X., Hu, L., and He, M.-X.: Scattering by pure seawater: Effect of salinity, Opt. Express, 17, 5698–5710, 2009.

Zhang, X., Twardowski, M., and Lewis, M.: Retrieving composition and sizes of oceanic particle subpopulations from the volume scattering function, Appl. Optics, 50, 1240–1259, 2011.

Zhang, X., Gray, D., Huot, Y., You, Y., and Bi, L.: Comparison of optically derived particle size distributions: scattering over the full angular range versus diffraction at near forward angles, Appl. Optics, 51, 5085–5099, 2012.